Chemical Methodologies 8(2024) 316-328

Chemical Methodologies

Journal homepage: http://chemmethod.com

Original Article

Voltammetric Sensor for Acyclovir Determination Based on $MoSe_2$/rGO Nanocomposite Modified Electrode

Somayeh Tajik[1,*], Fraiba Garkani Nejad[2], Reza Zaimbashi[2], Hadi Beitollahi[2]

[1]*Research Center of Tropical and Infectious Diseases, Kerman University of Medical Sciences, Kerman P.O. Box 76169-13555, Iran*
[2]*Environment Department, Institute of Science and High Technology and Environmental Sciences, Graduate University of Advanced Technology, Kerman, Iran*

ARTICLEINFO

Article history
Submitted: 2024-02-18
Revised: 2024-03-24
Accepted: 2024-04-10

ID: CHEMM-2402-1771
Checked for Plagiarism: Yes
Language check: Yes

DOI: 10.48309/CHEMM.2024.444547.1771

KEYWORDS
Screen printed graphite electrode
Electrochemical sensor
$MoSe_2$/rGO nanocomposite
Acyclovir

ABSTRACT

In this study, $MoSe_2$/rGO nanocomposite modified screen printed graphite electrode (SPGE) was designed for acyclovir (ACV) determination. The electrochemical investigation and measurement of ACV were performed by applying some voltammetric techniques and chronoamperometry. After modification of SPGE, the enhancement of the voltammetric response and the reduction of overpotential of ACV confirmed the good electrocatalytic ability of $MoSe_2$/rGO/SPGE sensor towards the ACV oxidation. The voltammetric method (differential pulse voltammetry (DPV)) was used to investigate the determination ability of $MoSe_2$/rGO nanocomposite/SPGE towards ACV determination under the optimum parameters and conditions. The $MoSe_2$/rGO/SPGE sensor indicated appreciable sensing ability towards ACV, with an optimal linear response from 0.03-190.0 μM and a limit of detection (LOD) of 0.01 μM. More importantly, the practical applicability of the designed sensor was confirmed in the ACV quantification in ACV tablet and urine samples, showing its potential application for real sample analysis.

* Corresponding author: Somayeh Tajik
E-mail: tajik_s1365@yahoo.com

GRAPHICAL ABSTRACT

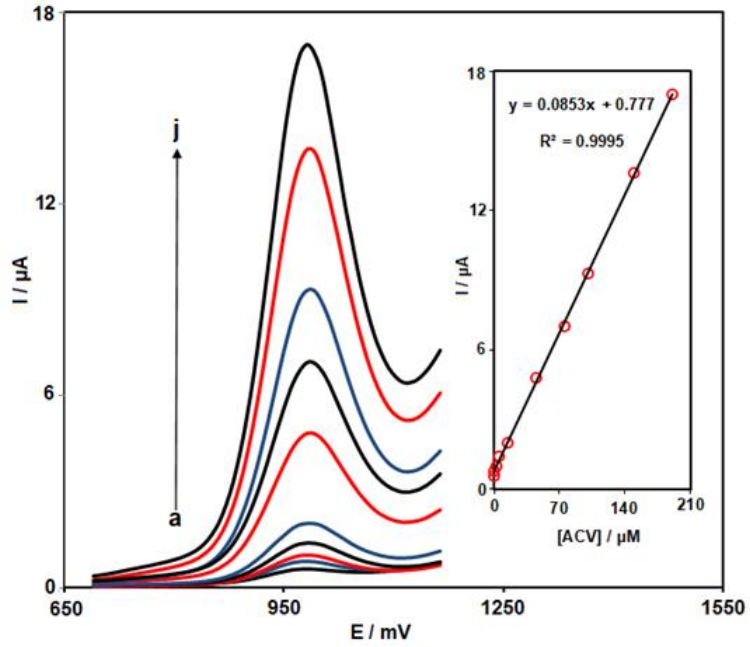

A novel electrochemical sensor for determination of acyclovir was constructed

Introduction

In last years, the swift emergence of viral diseases has been recognized as a serious threat to both human and veterinary health [1]. More recently, the viral diseases surpassed other infectious diseases to become the leading cause of death worldwide. This evolution has made viral diseases a paramount concern for public health. Acyclovir (ACV) is known as a synthetic nucleoside analog of purine derived from guanine. However, it differs from guanine in that it lacks a 3'-hydroxyl on its side chain. It has been extensively utilized in the clinical treatment of various viral diseases, including Epstein-Barr virus, varicella-zoster virus (VZV), hepatitis B virus (HBV), and herpes simplex virus (HSV). This medication has demonstrated remarkable therapeutic benefits in treating viral diseases such as cold sores, encephalitis, infections of central nervous system, keratitis, and corneal blindness [2,3]. When present in high concentrations in the body, ACV can cause adverse effects such as nausea and diarrhea. In addition, high doses of this medication can potentially cause serious side effects related to the kidneys and low platelet counts [4,5]. Therefore, the necessity of using a powerful analytical tool with high selectivity and sensitivity, and quick response is clearly evident for ACV determination in pharmaceutical compounds and biological samples. So far, several analytical techniques have been reported for the ACV detection, including spectrophotometry [6], radioimmunoassay [7], capillary electrophoresis [8], and chromatography [9,10], and. Despite being well-established and widely accepted for detecting ACV, these methods often encounter limitations such as expensive equipment, extensive sample preparation, the need for specialized expertise, and time-consuming procedures. These factors can render these methods unsuitable for routine analysis in clinical settings and can restrict their availability to healthcare professionals and patients. Due to their sensitivity, simplicity, rapid response and inexpensive instrumentation, electrochemical methods based on chemically modified electrodes (CMEs) present a promising alternative [11-21].

Research indicates that the screen-printing technology commonly employed in microelectronics holds significant value in producing electrodes for disposable

electrochemical (bio) sensors. Screen-printed electrodes (SPEs) offer a range of benefits such as simplified operation, adaptability, cost-effectiveness, portability, reliability, reduced dimensions, and scalability for mass production [22,23]. Consequently, it finds extensive utility within the realm of electroanalytical chemistry. Furthermore, the implementation of an SPE eliminates the need for meticulous cleaning procedures that traditional electrodes, such as glassy carbon electrodes, require. This innovation addresses the limitations inherent in conventional electrode systems, which necessitate frequent recalibration, lack stability, and prove unsuitable for on-site analyses due to their lengthy completion times spanning several hours. Furthermore, traditional electrode systems mandate the expertise of skilled professionals due to their complex isolation and washing protocols. Consequently, the shortcomings associated with traditional electrode systems have rendered them less effective compared to the advantages offered by SPEs. Nanotechnology, as one of the top advances of recent decades, has rapidly become one of the most important research and application fields in various domains [24-29]. More importantly, nanotechnology has a huge potential in the design, fabrication, and development of novel and practical sensors [30-37]. With the development of the nanostructures application in electrochemical sensors, it is known that the use of nanostructures to modify the surface of the electrode leads to the improvement of the speed of the electron transfer process, reduction of overvoltage and increase of the efficiency of the electrode [38-43].

Recently, there has been significant attention in research towards molybdenum-based two-dimensional transition metal dichalcogenides (2D nanomaterials) owing to their amazing physical and chemical attributes such as substantial surface area, heightened electronic conductivity, remarkable specific capacitance, their layered structure, inexpensive price, outstanding electrocatalytic activity, and good chemical stability [44,45]. Typically, chalcogenides like MoX_2 (where, X = S and Se) are synthesized to exhibit a two-dimensional layered configuration similar to graphite. The individual MoX_2 layer comprises a covalently bonded arrangement of Mo elements with chalcogenide elements. These layers are held together through gentle interactions (Van der Waals). $MoSe_2$ surpasses MoS_2 in terms of electrical conductivity and electrocatalytic performance due to its elevated metallic attributes and the presence of actively catalytic unsaturated selenium edges [46-48]. Nonetheless, the inert nature of the exposed planes on $MoSe_2$ nanosheets limits their reactivity, as the active sites crucial for catalysis are primarily concentrated along the unsaturated selenium edges. Therefore, due to the sparse distribution of these active edge sites, the overall electrocatalytic activity of $MoSe_2$ remains unsatisfactory. To tackle these limitations, $MoSe_2$ has been employed in conjunction with highly conductive carbonaceous materials, resulting in an enhancement of both $MoSe_2$'s conductivity and electrocatalytic activity. Because of its exceptional capacity to enhance electron transfer and its extensive surface area, reduced graphene oxide (rGO) can be readily combined with two-dimensional nanosheets like $MoSe_2$ to create heterostructures [49,50].

Concerning the aforementioned factors, the present investigation introduces the utilization of a novel and disposable sensor for the detection of ACV. This sensor capitalizes on the enhancement of the SPGE surface through the incorporation of a $MoSe_2$/rGO nanocomposite. Notably, the $MoSe_2$/rGO nanocomposite exhibited good electrocatalytic performance towards the ACV determination. This was evidenced by its notably narrow LOD, impressive sensitivity, and minimal over-voltage requirements. The resultant sensor was effectively employed for the quantification of ACV in urine samples and ACV tablets.

Experimental

Equipments and Reagents

The PGSTAT 302N Autolab (Metrohm, the Netherlands) operated by GPES software and connected to personal PC was applied to perform all electrochemical experiments. The pH control of phosphate buffer solution (PBSs) was measured by using a Metrohm 713 pH meter. The analytical grade of reagents with high purity were used in the present work as provided from Merck and Sigma-Aldrich companies without any further processing. The synthesis and characterization of $MoSe_2$/rGO nanocomposite has been given in our previously reported work [51]. Figure 1 displays its FE-SEM image.

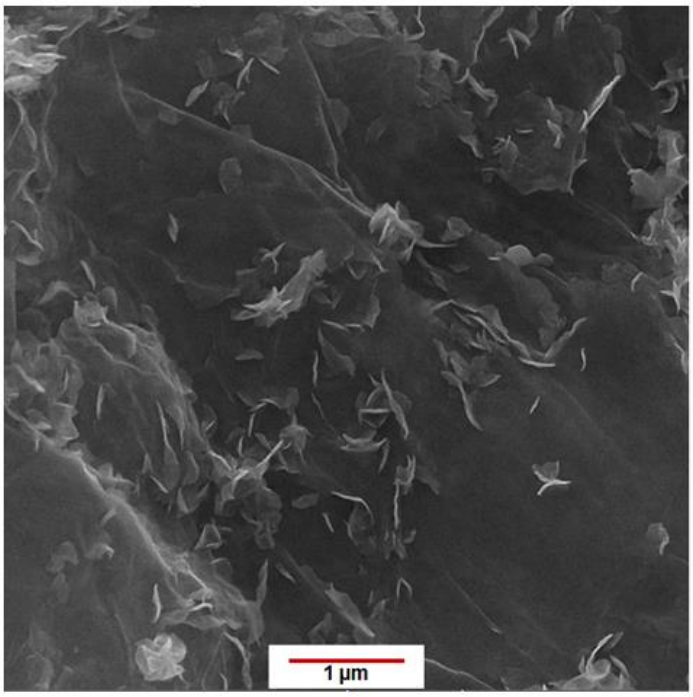

Figure 1: FE-SEM image of $MoSe_2$/rGO nanocomposite

Preparation of the $MoSe_2$/rGO Nanocomposite Modified SPGE

The procedure for SPGE modification is as follow: 1.0 mg of $MoSe_2$/rGO was initially subjected to ultrasonication for at least 20 min in 1 mL of solvent to prepare $MoSe_2$/rGO suspension, and then $MoSe_2$/rGO suspension (4.0 µL) was dropped carefully on the SPGE surface. After drying at room temperature, the $MoSe_2$/rGO/SPGE sensor was prepared.

The surface areas of unmodified SPGE and $MoSe_2$/rGO/SPGE were calculated to determine the effect of modification process. Accordingly, the CVs at various scan rates were recorded for 0.1 M KCl solution containing 1.0 mM $K_3[Fe(CN)_6]$. The Randles-Sevcik equation was used to calculate the surface areas. The $MoSe_2$/rGO/SPGE demonstrated an effective surface area (0.113 cm^2), which was 3.6 times greater than the surface area on unmodified electrode.

Results and Discussion

Investigating the Performance of the $MoSe_2$/rGO on the ACV Determination

The pH of buffer solution is a key parameter in electroanalysis of compounds. Therefore, the effect of pH in the present work was investigated in PBS (0.1 M) with various values of pH from 4.0 to 9.0 containing 75.0 µM ACV at $MoSe_2$/rGO/SPGE. From the voltammograms, the current responses of ACV enhanced with the increasing in pH value from 4.0 to 7.0, and then decreased at pH values higher than 7.0.

Therefore, the selected optimal buffer solution is PBS 0.1 M at pH 7.0 due to the highest peak current of ACV in this pH. The oxidation mechanism of ACV is presented in Scheme 1.

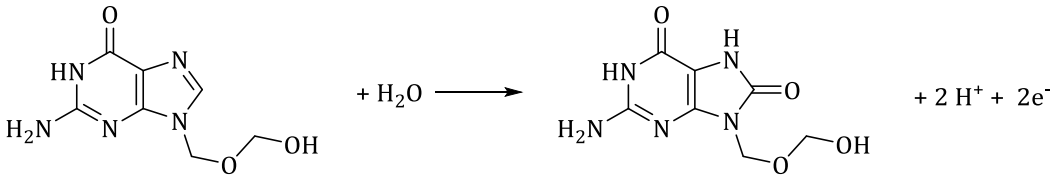

Scheme 1: The oxidation mechanism of ACV

To confirm the electrocatalytic response of prepared sensor ($MoSe_2$/rGO/SPGE) towards the electrochemical reaction of ACV, the CV responses of 100.0 µM ACV in PBS (0.1 M-pH 7.0) were recorded at various electrodes (unmodified SPGE (Figure 2 (voltammogram a)) and $MoSe_2$/rGO/SPGE (Figure 2 (voltammogram b)) at a scan rate of 50 mV.s^{-1}. From the obtained voltammograms, it is obvious that the observed electrochemical process is an irreversible process, because only one well-defined oxidation peak was obtained due to the ACV presence. Also, a weak oxidation peak with low Ipa was observed for ACV at bare SPGE (voltammogram a). In contrast, the SPGE surface modified with a nanocomposite of $MoSe_2$/rGO (voltammogram b) exhibited a notably amplified Ipa = 9.35 µA) and a shifted Epa toward negative values (Epa = 990 mV) in the presence of ACV, compared to the bare SPGE. This prominent enhancement in the oxidation peak characteristics can be ascribed to the remarkable impacts of the $MoSe_2$ and rGO sheets and their synergistic effects in the ACV oxidation.

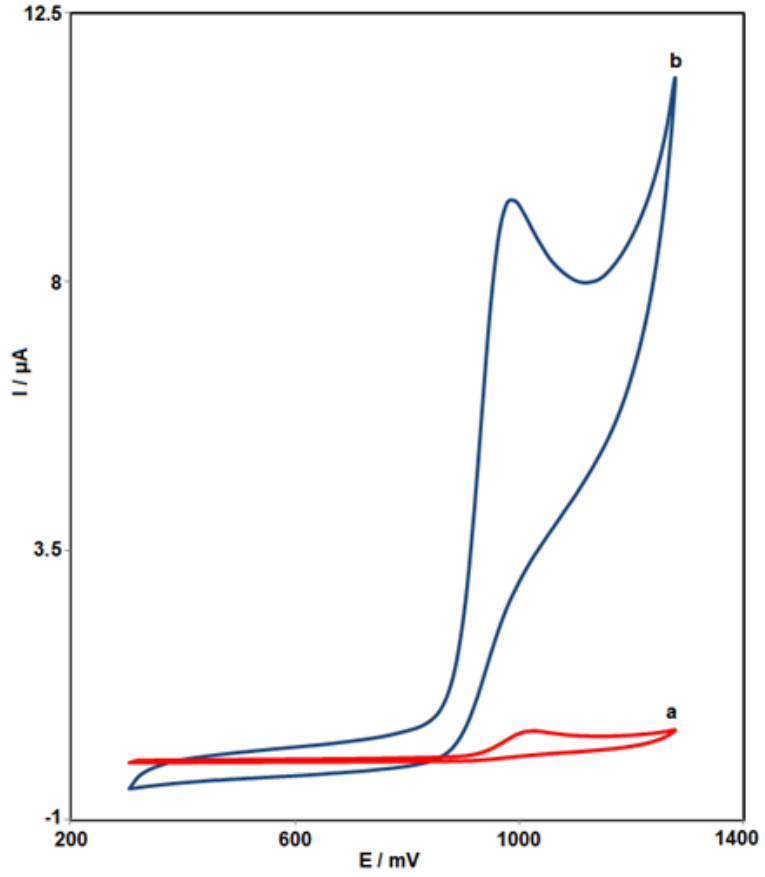

Figure 2: CVs of bare SPGE (a) and $MoSe_2$/rGO/SPGE (b) in 0.1 M PBS at pH 7.0 containing 100.0 µM ACV at 50 mV s^{-1} scan rate

Effect of Scan Rate

In addition, the effect of scan rate (υ) on ACV oxidation was evaluated using LSV on the $MoSe_2$/rGO/SPGE in PBS (0.1 M at pH 7.0) containing 90.0 µM ACV at various scan rates (10 to 300 $mV.s^{-1}$) (Figure 3). Figure 3 illustrates that the Ipa of ACV was increased with increasing of scan rates. Moreover, the data presented in Inset of Figure 3 shows a strong linear dependence between the Ipa and the $\upsilon^{1/2}$ within the range of 10-300 $mV.s^{-1}$ (Ipa (µA) = $1.6473\upsilon^{1/2}$ $(mV\ s^{-1})^{1/2}$ - 2.2396 (R^2 = 0.9991)), which suggests a diffusion-controlled process on the $MoSe_2$/rGO/SPGE surface.

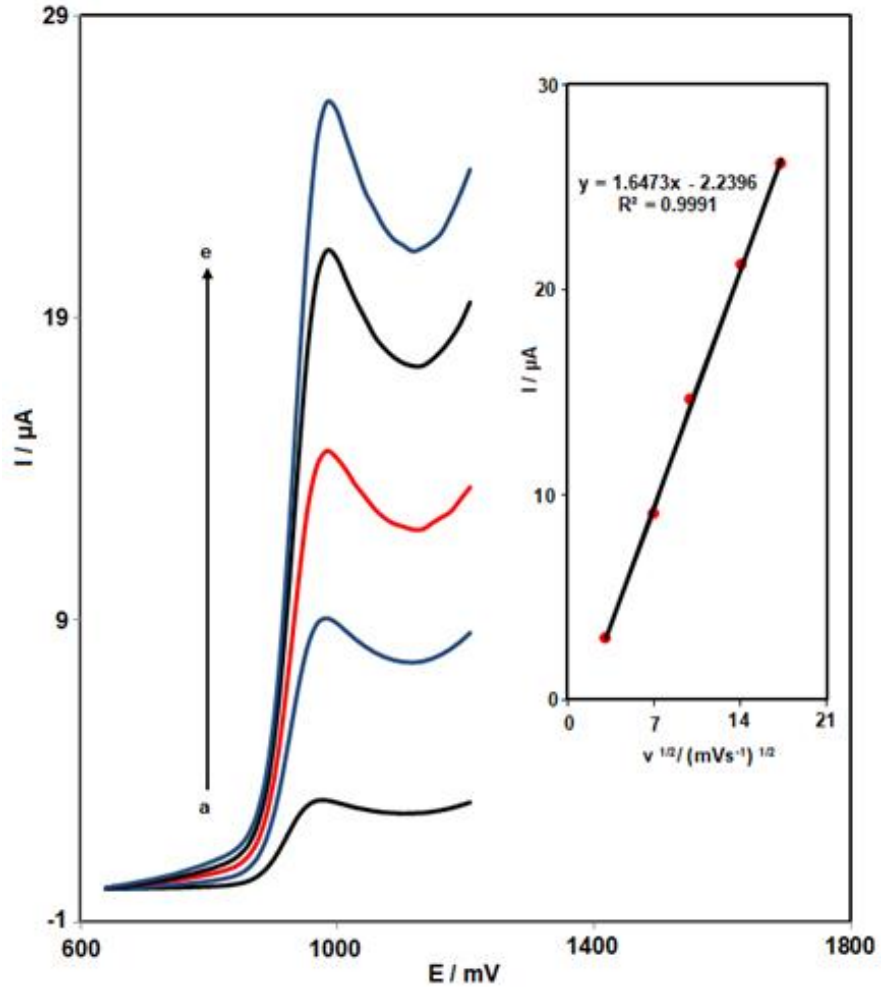

Figure 3: LSVs of $MoSe_2$/rGO/SPGE in 0.1 M PBS at pH 7.0 containing 90.0 µM ACV at different scan rates ((a) 10, (b) 50, (c) 100, (d) 200, and (e) 300 $mV\ s^{-1}$. Inset: the corresponding plot of Ipa (µA) vs. $\nu^{1/2}$ $(mV\ s^{-1})^{1/2}$

Chronoamperometric Measurements of ACV

A chronoamperometric investigation was conducted to determine the diffusion coefficient (D) of ACV at the $MoSe_2$/rGO/SPGE. The results of this investigation are depicted in Figure 4, which illustrates the obtained chronoamperograms for ACV at various concentrations in a pH 7.0 PBS. The reaction of an electroactive substance with a D is described by Cottrell's equation when the process is constrained by mass transport. In Figure 4A, a linear correlation is obtained between the current (I) and the square root of time ($t^{1/2}$) for the oxidation of varying ACV concentrations. The slopes obtained from the linear fits were then correlated with the different ACV concentrations, as demonstrated in Figure 4B. By utilizing the plotted slope in conjunction with the Cottrell equation, the D of ACV was calculated to be 2.1×10^{-5} cm^2/s.

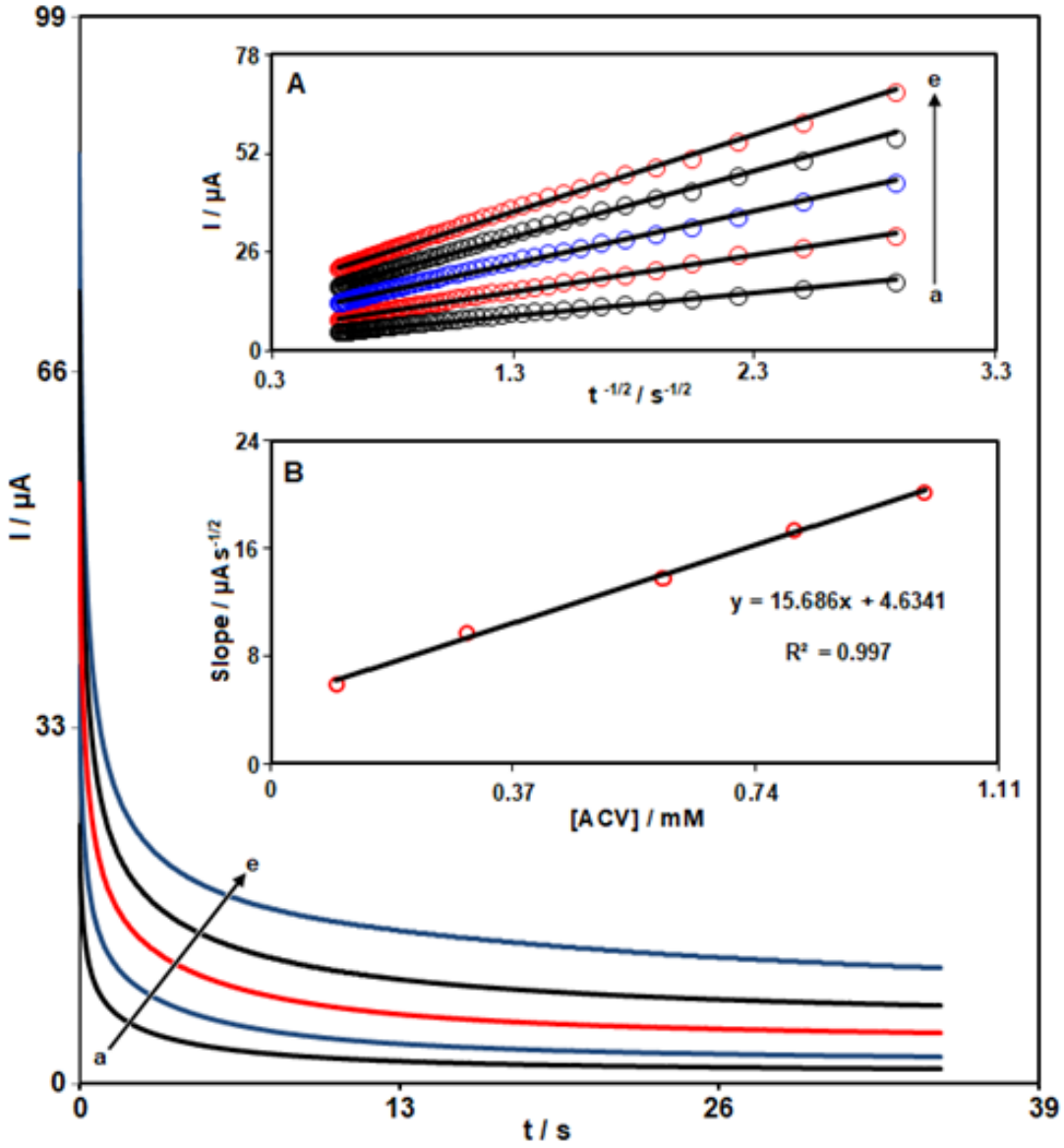

Figure 4: Chronoamperometric responses of $MoSe_2$/rGO/SPGE in 0.1 M PBS at pH 7.0 containing ACV at different concentrations ((a 0.1), (b 0.3), (c 0.6), (d 0.8), and (e 1.0 mM) of ACV). Insets: corresponding plots of I (µA)-$t^{-1/2}$ ($s^{-1/2}$) curves from the chronoamperograms (A) and corresponding plots of obtained slopes-[ACV]

Quantitative Analysis of ACV by DPV

Figure 5 demonstrates the DPV responses for ACV at different concentrations in PBS (0.1 M-pH 7.0) at the $MoSe_2$/rGO/SPGE in the following conditions: step potential (0.01 V) and pulse amplitude (0.025 V). It was found that the Ipa of ACV increased proportionally along with increasing in ACV concentration over a range of 0.03 µM to 190.0 µM. Likewise, by plotting the Ipa of ACV vs. its concentrations a good linearity was obtained (Ipa (µA) = $0.0853C_{ACV}$ (µM) + 0.777 (R^2 = 0.9995)) (Figure 5-Inset). The LOD value was obtained to be 0.01 µM. In addition, the performance of $MoSe_2$/rGO/SPGE sensor was compared with some of reported electrochemical sensors for ACV determination (Table 1).

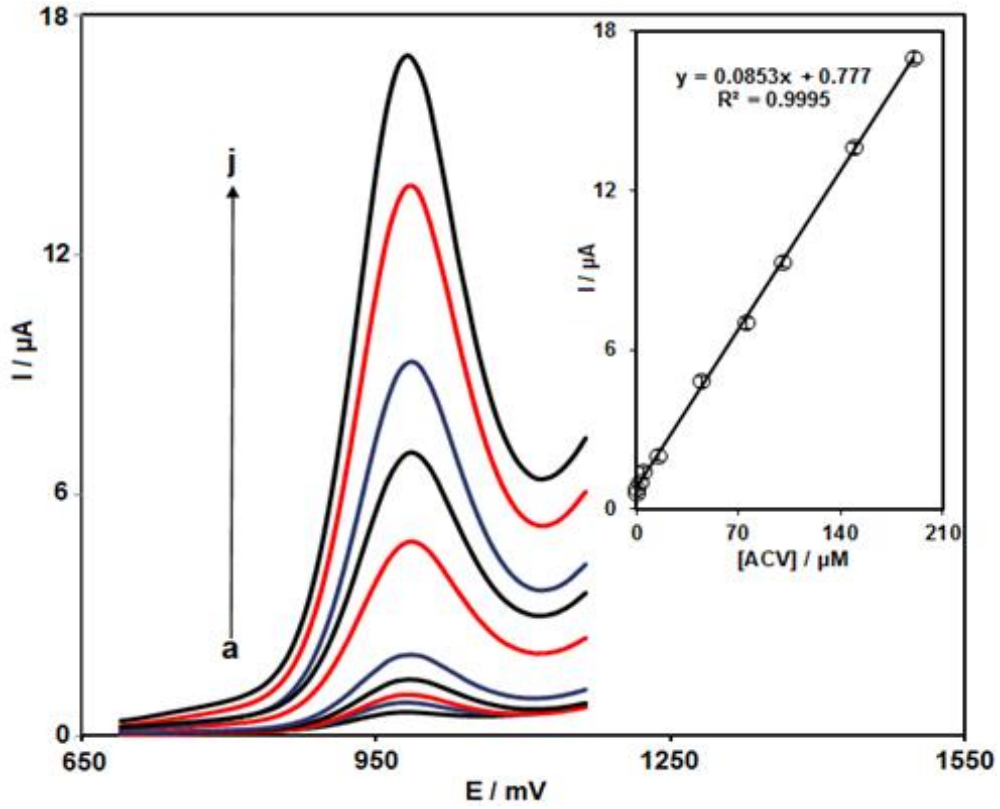

Figure 5: DPVs of $MoSe_2$/rGO/SPGE in 0.1 M PBS at pH 7.0 containing various concentrations of ACV ((a) 0.03, (b) 0.3, (c) 2.5, (d) 5.0, (e) 15.0, (f) 45.0, (g) 75.0, (h) 100.0, (i) 150.0, and (j) 190.0 µM). Inset: The linear plot of Ipa (µA) vs. C_{ACV} (µM)

Table 1: The performance of $MoSe_2$/rGO/SPGE sensor in comparison with some of previous reported electrochemical sensors for ACV determination

Electrochemical Sensor	Electrochemical Method	Linear Range	LOD	Ref.
Ca-doped ZnO nanoparticles (NPs)/GCE	Square wave voltammetry (SWV)	8.0×10^{-8}-2.4×10^{-5} M	6.18 nM	[11]
Reduced graphene oxide (rGO)-TiO_2-Au nanocomposite/glassy carbon electrode (GCE)	Linear sweep voltammetry (LSV)	1-100 µM	0.3 µM	[52]
Magnetic CdO NPs/carbon paste electrode (CPE)	DPV	1-100 µM	300 nM	[53]
Multiwalled carbon nanotube/iron-doped polypyrrole/GCE	LSV	0.03-10.0 µM	10.0 nM	[54]
Fullerene-C_{60}/GCE	DPV	9.0×10^{-8}-6.0×10^{-6} M	14.8 nM	[55]
$MoSe_2$/rGO/SPGE	DPV	0.03-190.0 µM	0.01 µM	This work

Stability Studies of $MoSe_2$/rGO/SPGE for ACV Determination

The stability studies of $MoSe_2$/rGO/SPGE sensor were done by recording the voltammetric response of this sensor towards 60.0 µM ACV over 12 days. The obtained results demonstrated that the voltammetric response retained 97.1% of its initial response after 12 days, indicating the good stability of the developed sensor.

Analytical Application of $MoSe_2$/rGO/SPGE for Determination of ACV in Real Samples

The urine samples and ACV tablets were used to investigate the practical applicability of the $MoSe_2$/rGO/SPGE for ACV determination by DPV. The recovery studies were done by standard addition method to confirm the accuracy by spiking the ACV tablet and urine samples with ACV in various concentrations (Table 2). The recovery values varied from 96.7% to 104.2%. Also, the results showed a good precision as can be inferred from the low values of RSD (%) obtained (n = 5).

Table 2: The determination results of ACV in urine samples and ACV tablets

Real sample	Added concentration in µM	Detected concentration in µM	Recovery (%)	R.S.D. (%)
ACV tablet	0	3.2	-	2.4
	2.0	5.1	98.1	3.3
	4.0	7.5	104.2	1.7
	6.0	9.1	98.9	2.6
	8.0	11.3	100.9	2.1
Urine	0	-	-	-
	5.0	5.1	102.0	2.4
	7.0	6.9	98.6	3.0
	9.0	8.7	96.7	2.0
	11.0	11.1	100.9	2.7

Conclusion

In the presented study, a facile and novel $MoSe_2$/rGO-modified SPGE was designed and applied for sensitive and accurate determination of ACV. With the synergistic effect from $MoSe_2$ and rGO sheets, the designed sensor exhibited good performance for oxidation of ACV by reducing the over-potential and enhancing the current response. In addition, the $MoSe_2$/rGO/SPGE sensor exhibited analytical performances for determining ACV, including wide response range (0.03 µM to 190.0 µM), low LOD (0.01µM), and high sensitivity (0.0853 $\mu A.\mu M^{-1}$). Also, $MoSe_2$/rGO/SPGE sensor demonstrated good stability for ACV determination. Finally, the designed sensor was successfully utilized for ACV determination in ACV tablet and urine samples, with high reliability and accuracy.

Acknowledgement

This study was financially supported by the Research Center of Tropical and Infectious Diseases, Kerman University of Medical Sciences, Kerman, Iran (grant number: 401000924 research ethics committees' code: IR.KMU.REC.1401.552). The APC was funded by A.D.B.

ORCID

Hadi Beitollahi
https://orcid.org/0000-0002-0669-5216

References

[1]. Howard C.R., Fletcher N.F., Emerging virus diseases: can we ever expect the unexpected?, *Emerging Microbes & Infections*, 2012, **1**:1 [Crossref], [Google Scholar], [Publisher]
[2]. Clercq E.D., Antivirals and antiviral strategies, *Nature Reviews Microbiology*, 2004, **2**:704 [Crossref], [Google Scholar], [Publisher]
[3]. Jiang Y.C., Feng H., Lin Y.C., Guo X.R., New strategies against drug resistance to herpes simplex virus, *International Journal of Oral Science*, 2016, **8**:1 [Crossref], [Google Scholar], [Publisher]
[4]. Adair J., Gold M., Bond R., Acyclovir neurotoxicity: clinical experience and review of the literature, *Southampton Medical Journal*,

1994, **87**:1227 [Crossref], [Google Scholar], [Publisher]
[5]. Singla P., Singh O., Chabba S., Mahajan R.K., Pluronic-SAILs (surface active ionic liquids) mixed micelles as efficient hydrophobic quercetin drug carriers, *Journal of Molecular Liquids*, 2018, **249**:294 [Crossref], [Google Scholar], [Publisher]
[6]. Yu L., Xiang B., Quantitative determination of acyclovir in plasma by near infrared spectroscopy, *Microchemical Journal,* 2008, **90**:63 [Crossref], [Google Scholar], [Publisher]
[7]. Tadepalli S.M., Quinn R.P., Scintillation proximity radioimmunoassay for the measurement of acyclovir, *Journal of Pharmaceutical and Biomedical Analysis*, 1996, **15**:157 [Crossref], [Google Scholar], [Publisher]
[8]. Vo H.C., Henning P.A., Leung D.T., Sacks S.L., Development and validation of a plasma assay for acyclovir using high-performance capillary electrophoresis with sample stacking, *Journal of Chromatography B*, 2002, **772**:291 [Crossref], [Google Scholar], [Publisher]
[9]. Sasanya J.J., Abd-Alla A.M.M., Parker A.G., Cannavan A., Analysis of the antiviral drugs acyclovir and valacyclovir-hydrochloride in tsetse flies (Glossina pallidipes) using LC–MSMS, *Journal of Chromatography B,* 2010, **878**:2384 [Crossref], [Google Scholar], [Publisher]
[10]. Tzanavaras P.D., Themelis D.G., High-throughput HPLC assay of acyclovir and its major impurity guanine using a monolithic column and a flow gradient approach, *Journal of Pharmaceutical and Biomedical Analysis,* 2007, **43**:1526 [Crossref], [Google Scholar], [Publisher]
[11]. Ilager D., Shetti N.P., Malladi R.S., Shetty N.S., Reddy K.R., Aminabhavi T.M., Synthesis of Ca-doped ZnO nanoparticles and its application as highly efficient electrochemical sensor for the determination of anti-viral drug, acyclovir, *Journal of Molecular Liquids*, 2021, **322**:114552 [Crossref], [Google Scholar], [Publisher]
[12]. Lotfi Z., Gholivand M.B., Shamsipur M., An electrochemical sensor based on Ag nanoparticles decorated on cadmium sulfide nanowires/reduced graphene oxide for the determination of acyclovir, *Journal of Alloys and Compounds*, 2022, **903**:163912 [Crossref], [Google Scholar], [Publisher]
[13]. Abedini S., Rafati A.A., Ghaffarinejad A., A simple and low-cost electrochemical sensor based on a graphite sheet electrode modified by carboxylated multiwalled carbon nanotubes and gold nanoparticles for detection of acyclovir, *New Journal of Chemistry*, 2022, **46**:20403 [Crossref], [Google Scholar], [Publisher]
[14]. Beitollahi H., Tajik S., Mohammadi S.Z., Baghayeri M., Voltammetric determination of hydroxylamine in water samples using a 1-benzyl-4-ferrocenyl-1*H*-[1, 2, 3]-triazole/carbon nanotube-modified glassy carbon electrode, *Ionics*, 2014, **20**:571 [Crossref], [Google Scholar], [Publisher]
[15]. Ardakani M.M., Taleat Z., Beitollahi H., Salavati-Niasari M., Mirjalili B.B.F., Taghavinia N., Electrocatalytic oxidation and nanomolar determination of guanine at the surface of a molybdenum (VI) complex–TiO_2 nanoparticle modified carbon paste electrode, *Journal of Electroanalytical Chemistry*, 2008, **624**:73 [Crossref], [Google Scholar], [Publisher]
[16]. Karimi-Maleh H., Darabi R., Karimi F., Karaman C., Shahidi S.A., Zare N., Baghayeri M., Fu L., Rostamnia S., Rouhi J., State-of-art advances on removal, degradation and electrochemical monitoring of 4-aminophenol pollutants in real samples: A review, *Environmental Research,* 2023, **222**:115338 [Crossref], [Google Scholar], [Publisher]
[17]. Raoof J.B., Ojani R., Beitollahi H., Hosseinzadeh R., Electrocatalytic oxidation and highly selective voltammetric determination of L-cysteine at the surface of a 1-[4-(ferrocenyl ethynyl) phenyl]-1-ethanone modified carbon paste electrode, *Analytical Sciences*, 2006, **22:**1213 [Crossref], [Google Scholar], [Publisher]
[18]. Ariavand S., Ebrahimi M., Foladi E., Design and construction of a novel and an efficient potentiometric sensor for determination of sodium ion in urban water samples, *Chemical Methodologies,* 2022, **6**:886 [Crossref], [Google Scholar], [Publisher]
[19]. Cheraghi S., Taher M.A., Karimi-Maleh H., Karimi F., Shabani-Nooshabadi M., Alizadeh M., Al-Othman A., Erk N., Raman P.K.Y., Karaman C., Novel enzymatic graphene oxide based biosensor for the detection of glutathione in biological body

fluids, *Chemosphere,* 2022, **287**:132187 [Crossref], [Google Scholar], [Publisher]
[20]. Roshanfekr H., A simple specific dopamine aptasensor based on partially reduced graphene oxide–Au NPs composite, *Progress in Chemical and Biochemical Research*, 2023, **6**:61 [Crossref], [Google Scholar], [Publisher]
[21]. Karimi-Maleh H., Liu Y., Li Z., Darabi R., Orooji Y., Karaman C., Karimi F., Baghayeri M., Rouhi J., Fu L., Calf thymus ds-DNA intercalation with pendimethalin herbicide at the surface of ZIF-8/Co/rGO/C_3N_4/ds-DNA/SPCE; A bio-sensing approach for pendimethalin quantification confirmed by molecular docking study, *Chemosphere*, 2023, **332**:138815 [Crossref], [Google Scholar], [Publisher]
[22]. Singh A.K., Agrahari S., Gautam R.K., Tiwari I., Fabrication of a novel screen-printed carbon electrode based disposable sensor for sensitive determination of an endocrine disruptor BPSIP in environmental and biological matrices, *Microchemical Journal*, 2023, **193**:109031 [Crossref], [Google Scholar], [Publisher]
[23]. Razavi R., Garkani Nejad F., Ahmadi S.A., Beitollahi H., Synthesis of ZnO@TiO_2 nanoparticles and its application to construct an electrochemical sensor for determination of hydrazine, *Electrochemistry Communications,* 2024, **159**:107639 [Crossref], [Google Scholar], [Publisher]
[24]. Janitabar Darzi S., Bastami H., Au decorated mesoporous TiO_2 as a high performance photocatalyst towards crystal violet dye, *Advanced Journal of Chemistry-Section A*, 2022, **5**:22 [Crossref], [Google Scholar], [Publisher]
[25]. Zhang J., Wu Z., Zhan S., Li M., Wang Y., Xu H., Gao J., Nano-carrier polyamidoamine dendrimer G4 induces mitochondrialdependent apoptosis in human multidrug-resistant breast cancer cells through G0/G1 phase arrest, *Current Pharmaceutical Biotechnology*, 2023, **24**:589 [Crossref], [Google Scholar], [Publisher]
[26]. Mhaibes R.M., Arzehgar Z., Mirzaei Heydari M., Fatolahi L., ZnO Nanoparticles: A Highly Efficient and Recyclable Catalyst for Tandem Knoevenagel- Michael- Cyclocondensation Reaction, *Asian Journal of Green Chemistry*, 2023, **7**:1 [Crossref], [Google Scholar], [Publisher]
[27]. Alinezhad H., Hajiabbas Tabar Amiri P., Mohseni Tavakkoli S., Muslim Muhiebes R., Fakri Mustafa Y., Progressive types of Fe_3O_4 nanoparticles and their hybrids as catalysts, *Journal of Chemical Reviews,* 2022, **4**:288 [Crossref], [Google Scholar], [Publisher]
[28]. Alao I.I., Peter Oyekunle I., Iwuozor K.O., Chizitere Emenike E., Green synthesis of copper nanoparticles and investigation of its antimicrobial properties, *Advanced Journal of Chemistry-Section B*, 2022, **4**:39 [Crossref], [Publisher]
[29]. Baghernejad B., Alikhani M., Nano-cerium oxide/aluminum oxide as an efficient catalyst for the synthesis of xanthene derivatives as potential antiviral and anti-inflammatory agents*, Journal of Applied Organometallic Chemistry,* 2022, **2**:140 [Crossref], [Google Scholar], [Publisher]
[30]. Singh A., Sharma A., Arya S., Electrochemical sensing of ascorbic acid (AA) from human sweat using Ni–SnO_2 modified wearable electrode, *Inorganic Chemistry Communications*, 2023, **152**:110718 [Crossref], [Google Scholar], [Publisher]
[31]. Mazloum-Ardakani M., Beitollahi H., Ganjipour B., Naeimi H., Novel carbon nanotube paste electrode for simultaneous determination of norepinephrine, uric acid and d-penicillamine, *International Journal of Electrochemical Science*, 2010, **5**:531 [Crossref], [Google Scholar], [Publisher]
[32]. Mehdizadeh Z., Shahidi S., Ghorbani-Hasan Saraei A., Limooei M., Bijad M., Monitoring of amaranth in drinking samples using voltammetric amplified electroanalytical sensor, *Chemical Methodologies*, 2022, **6**:246 [Crossref], [Google Scholar], [Publisher]
[33]. Zhang Z., Karimi-Maleh H., In situ synthesis of label-free electrochemical aptasensor-based sandwich-like AuNPs/PPy/$Ti_3C_2T_x$ for ultrasensitive detection of lead ions as hazardous pollutants in environmental fluids, *Chemosphere*, 2023, **324**:138302 [Crossref], [Google Scholar], [Publisher]
[34]. Zhang Z., Karimi-Maleh H., Label-free electrochemical aptasensor based on gold nanoparticles/titanium carbide MXene for lead detection with its reduction peak as index signal,

Advanced Composites and Hybrid Materials, 2023, **6**:68 [Crossref], [Google Scholar], [Publisher]
[35]. Kazemipour M., Ansari M., Mohammadi A., Beitollahi H., Ahmadi, R., Use of adsorptive square-wave anodic stripping voltammetry at carbon paste electrode for the determination of amlodipine besylate in pharmaceutical preparations, *Journal of Analytical Chemistry*, 2009, **64**:65 [Crossref], [Google Scholar], [Publisher]
[36]. Tajik S., Beitollahi H., Dourandish Z., Mohammadzadeh Jahani P., Sheikhshoaie I., Askari M.B., Salarizadeh P., Garkani Nejad F., Kim D., Kim S.Y., Varma R.S., Shokouhimehr M., Applications of non‐precious transition metal oxide nanoparticles in electrochemistry, *Electroanalysis*, 2022, **34**:1065 [Crossref], [Google Scholar], [Publisher]
[37]. Bijad M., Karimi-Maleh H., Farsi M., Shahidi S.A., An electrochemical-amplified-platform based on the nanostructure voltammetric sensor for the determination of carmoisine in the presence of tartrazine in dried fruit and soft drink samples, *Journal of Food Measurement and Characterization*, 2018, **12**:634 [Crossref], [Google Scholar], [Publisher]
[38]. Peyman H., Design and fabrication of modified DNA-Gp nano-biocomposite electrode for industrial dye measurement and optical confirmation, *Progress in Chemical and Biochemical Research,* 2022, **5**:391 [Crossref], [Google Scholar], [Publisher]
[39]. Chakraborty U., Kaur I., Chauhan A., Kaur N., Kaur G., Chaudhary G.R., Zinc oxide-copper sulfide semiconductor nano-heterostructure for low-level electrochemical detection of 4-nitrotoluene, *Electrochimica Acta*, 2023, **447**:142160 [Crossref], [Google Scholar], [Publisher]
[40]. Garkani Nejad F., Asadi M.H., Sheikhshoaie I., Dourandish Z., Zaimbashi R., Beitollahi H., Construction of modified screen-printed graphite electrode for the application in electrochemical detection of sunset yellow in food samples, *Food and Chemical Toxicology,* 2022, **166**:113243 [Crossref], [Google Scholar], [Publisher]
[41]. Karimi-Maleh H., Fakude C.T., Mabuba N., Peleyeju G.M., Arotiba O.A., The determination of 2-phenylphenol in the presence of 4-chlorophenol using nano-Fe_3O_4/ionic liquid paste electrode as an electrochemical sensor, *Journal of Colloid and Interface Science*, 2019, **554**:603 [Crossref], [Google Scholar], [Publisher]
[42]. Buledi J.A., Mahar N., Mallah A., Solangi A.R., Palabiyik I.M., Qambrani N., Karimi F., Vasseghian Y., Karimi-Maleh H., Electrochemical quantification of mancozeb through tungsten oxide/reduced graphene oxide nanocomposite: a potential method for environmental remediation, *Food and Chemical Toxicology*, 2022, **161**:112843 [Crossref], [Google Scholar], [Publisher]
[43]. Beitollahi H., Tajik S., Dourandish Z., Garkani Nejad F., Simple preparation and characterization of hierarchical flower-like $NiCo_2O_4$ nanoplates: applications for sunset yellow electrochemical analysis, *Biosensors,* 2022, **12**:912 [Crossref], [Google Scholar], [Publisher]
[44]. Tedstone A.A., Lewis D.J., O'Brien P., Synthesis, properties, and applications of transition metal-doped layered transition metal dichalcogenides, *Chemistry of Materials*, 2016, **28**:1965 [Crossref], [Google Scholar], [Publisher]
[45]. Yang L., Zhou W., Lu J., Hou D., Ke Y., Li G., Tang Z., Kang X., Chen S., Hierarchical spheres constructed by defect-rich MoS_2/carbon nanosheets for efficient electrocatalytic hydrogen evolution, *Nano Energy*, 2016, **22**:490 [Crossref], [Google Scholar], [Publisher]
[46]. Gao Y.P., Wu X., Huang K.J., Xing L.L., Zhang Y.Y., Liu L., Two-dimensional transition metal diseleniums for energy storage application: a review of recent developments, *CrystEngComm*, 2017, **19**:404 [Crossref], [Google Scholar], [Publisher]
[47]. Eftekhari A., Molybdenum diselenide ($MoSe_2$) for energy storage, catalysis, and optoelectronics. *Applied Materials Today*, 2017, **8**:1 [Crossref], [Google Scholar], [Publisher]
[48]. Lin S.H., Kuo J.L., Activating and tuning basal planes of MoO_2, MoS_2, and $MoSe_2$ for hydrogen evolution reaction, *Physical Chemistry Chemical Physics*, 2015, **17**:29305 [Crossref], [Google Scholar], [Publisher]
[49]. Wang Z., Yue H.Y., Yu Z.M., Yao F., Gao X., Guan E.H., Zhang H.J., Wang W.Q., One-pot hydrothermal synthesis of $MoSe_2$ nanosheets

spheres-reduced graphene oxide composites and application for high-performance supercapacitor, *Journal of Materials Science Materials in Electronics*, 2019, **30**:8537 [Crossref], [Google Scholar], [Publisher]
[50]. Liu Z.Q., Li N., Zhao H.Y., Du Y.P., Colloidally synthesized $MoSe_2$/graphene hybrid nanostructures as efficient electrocatalysts for hydrogen evolution, *Journal of Materials Chemistry A*, 2015, **3**:19706 [Crossref], [Google Scholar], [Publisher]
[51]. Hasanpour M., Pardakhty A., Tajik S., The development of disposable electrochemical sensor based on $MoSe_2$-rGO nanocomposite modified screen printed carbon electrode for amitriptyline determination in the presence of carbamazepine, application in biological and water samples, *Chemosphere*, 2022, **308**:136336 [Crossref], [Google Scholar], [Publisher]
[52]. Lu X.Y., Li J., Kong F.Y., Wei M.J., Zhang P., Li Y., Wang W., Improved performance for the electrochemical sensing of acyclovir by using the rGO–TiO_2–Au nanocomposite-modified electrode, *Frontiers in Chemistry*, 2022, **10:**892919 [Crossref], [Google Scholar], [Publisher]
[53]. Naghian E., Marzi Khosrowshahi E., Sohouli E., Pazoki-Toroudi H.R., Sobhani-Nasab A., Rahimi-Nasrabadi M., Ahmadi F., Electrochemical oxidation and determination of antiviral drug acyclovir by modified carbon paste electrode with magnetic CdO nanoparticles. *Frontiers in Chemistry*, 2020, **8:**689 [Crossref], [Google Scholar], [Publisher]
[54]. Shahrokhian S., Azimzadeh M., Amini M.K., Modification of glassy carbon electrode with a bilayer of multiwalled carbon nanotube/tiron-doped polypyrrole: Application to sensitive voltammetric determination of acyclovir. *Materials Science and Engineering: C*, 2015, **53**:134 [Crossref], [Google Scholar], [Publisher]
[55]. Shetti N.P., Malode S.J., Nandibewoor S.T., Electrochemical behavior of an antiviral drug acyclovir at fullerene-C_{60}-modified glassy carbon electrode. *Bioelectrochemistry*, 2012, **88**:76 [Crossref], [Google Scholar], [Publisher]

Use your device to scan and read the article online

HOW TO CITE THIS ARTICLE
S. Tajik, F. Garkani Nejad, R. Zaimbashi, H. Beitollahi. Voltammetric Sensor for Acyclovir Determination Based on $MoSe_2$/rGO Nanocomposite Modified Electrode. *Chem. Methodol.*, 2024, 8(5) 316-328
DOI: https://doi.org/10.48309/CHEMM.2024.444547.1771
URL: https://www.chemmethod.com/article_194063.html